ELSEVIER

Journal of Chromatography A, 781 (1997) 107–112

JOURNAL OF CHROMATOGRAPHY A

Peak shape distortions during capillary electrophoretic separations of multicomponent samples in two co-ion buffers

Robert L. Williams[a], Bart Childs[b], Eric V. Dose[c], Georges Guiochon[d], Gyula Vigh[a,*]

[a]*Chemistry Department, Texas A and M University, College Station, TX 77843-3255, USA*

[b]*Computer Science Department, Texas A and M University, College Station, TX 77843-3255, USA*

[c]*470 Clarendon Ave., Winter Park, FL 32789, USA*

[d]*Chemistry Department, University of Tennessee, Knoxville, TN 37996-1600, USA*

Abstract

During the capillary electrophoretic separation of a five-component quaternary ammonium analyte sample in two co-ion background electrolytes prepared from phosphoric acid, lithium hydroxide and tetrabutylammonium hydroxide, grossly distorted analyte peaks were observed. The electropherograms were successfully simulated using an earlier mathematical model of electrophoresis that was extended to handle up to eight nonprotic sample ions and two nonprotic background electrolyte co-ions. Peak shape distortion closely followed the predictions made during the recently described simulations of single analyte–two co-ion background electrolyte systems. Peak shape distortion was shown to depend on the relative mobilities of the particular analyte, the non-comigrating system peak and the governing co-ion. Severe peak shape distortion could occur in every multiple co-ion background electrolyte, such as in the indirect detection background electrolytes and charged interacting agent-containing background electrolytes, when certain analyte peaks and the non-comigrating system peaks overlap.

Keywords: Quaternary ammonium compounds; Computer simulation; Background electrolyte composition; Peak shape

1. Introduction

The deleterious effects of electromigration dispersion (EMD) were discovered [1,2] in the early days of capillary electrophoresis (CE), and efforts to mitigate its consequences or eliminate its sources have continued since [3–9]. In a recent paper [10] we described the results of a computer simulation study that was designed to reveal what happens when single, strong electrolyte analytes are electrophoresed in background electrolytes (BGEs) that contain a single, strong electrolyte counter ion and two strong electrolyte co-ions. The computer program first described in [11] was modified to accommodate two strong electrolyte co-ions in the BGE. The simulated BGEs contained a fast cation ($40 \cdot 10^{-5}$ cm^2/V s) and a slow cation ($20 \cdot 10^{-5}$ cm^2/V s) as co-ions. Their mol ratio was varied between 0 and 1 while the total co-ion concentration was maintained at 25 m*M*. Each single analyte was injected at a concentration of 1 m*M*; the analytes were dissolved in the respective 25 m*M* BGEs. The effective mobilities of the single analytes studied were (45; 38; 31; 22 and 15)$\cdot 10^{-5}$ cm^2/V s to evenly cover the mobility range of the co-ions. In each two co-ion BGE the analytes generated two system peaks: one of which co-migrated with the analyte (co-migrating system peak), the other did not co-migrate with any analyte (non-comigrating system peak). The classical peak shape rules of the single co-ion BGEs (i.e. when the

*Corresponding author.

0021-9673/97/$17.00
PII S0021-9673(97)00509-8

analyte is faster than the co-ion, the analyte peak fronts [1,11]) did not apply in the two co-ion BGEs. Extended peak shape rules could be derived by recognizing that the peak shape of the analyte was determined by its migration position between the closest migrating co-ion (governing co-ion) and the non-comigrating system peak. These rules state [10] that: (i) when the analyte is faster than or slower than all of the co-ions, the self-sharpening boundary of the analyte peak faces towards the mobility position of the co-ions; (ii) the self-sharpening boundary of an analyte that migrates between the governing co-ion and the non-comigrating system peak always faces towards the governing co-ion; (iii) the closer the analyte and the non-comigrating system peak are, the more defocused the diffuse boundary of the analyte peak is. It was found that when an analyte peak and a non-comigrating system peak began to overlap, the analyte peak became grossly defocused due to the accompanying "bow-tie" pattern of the local electric field strength.

The objective of the work reported in this paper was (i) to extend the simulation model further to allow it to simultaneously handle up to eight analytes in two co-ion BGEs, (ii) to test the applicability of the extended peak shape rules in systems with multiple analytes and (iii) to verify experimentally that the predicted peak patterns do indeed exist in real-life systems.

2. Experimental

A P/ACE 2100 CE system, equipped with a UV detector set to 214 nm and 57 cm (50 cm effective length)×50 μm I.D. eCAP Neutral capillaries (Part Number 477441) was used for the separations (Beckman Instruments, Fullerton, CA, USA). The cartridge coolant was thermostatted at 37°C, the outlet vial electrode was kept at the high positive potential and the field strength was set at 320 V/cm. (Power dissipation was kept below 750 mW/m). All analytes were dissolved at 1 m*M* concentration in the respective BGEs and pressure-injected by 1.5 p.s.i. nitrogen for 1 s (1 p.s.i.=6894.76 Pa). The BGEs were prepared by titrating 50 m*M* phosphoric acid solutions to pH 2.2 with lithium hydroxide or tetrabutylammonium hydroxide, or with a pre-made mixture of the two strong bases. Benzylalcohol was used as electroosmotic flow marker according to the pressure-assisted capillary electrophoretic method (PreMCE) developed in our laboratory [12], and all effective mobilities (μ^{eff}) were corrected for the linear potential ramp at the beginning of the separation [13]. Phosphoric acid, lithium hydroxide, tetrabutylammonium (TBA^+) hydroxide, benzyl alcohol and the chemicals used to synthesize test analytes (α-hydroxymethylbenzyl)trimethylammonium ($HMBTM^+$) bromide, (α-hydroxymethylbenzyl)triethylammonium ($HMBTE^+$) bromide and (α-hydroxymethylbenzyl)tributylammonium ($HMBTB^+$) bromide according to [14] were obtained from Aldrich (Milwaukee, WI, USA). Deionized water for the BGEs was prepared by a Milli-Q unit (Millipore, Milford, MA, USA). The μ^{eff} values used for Li^+ and TBA^+ were $40 \cdot 10^{-5}$ and $20 \cdot 10^{-5}$ cm^2/V s, respectively [10]. The effective mobility of the hypothetical strong electrolyte anion that had a mobility identical to that of $H_2PO_4^-$ under the experimental conditions was $-18 \cdot 10^{-5}$ cm^2/V s [10].

The original Fortran 90 simulation program [11] was modified to allow the modelling of up to 8 analyte ions and two BGE co-ions. The constant simulation parameters were: equivalent cell length= 1.5 μm, total capillary length=26 666 cells (corresponding to 4.0 cm), injector-to-detector capillary length=24 000 cells (corresponding to 3.6 cm), electroosmotic flow velocity=0.01 cm/s, initial time step=0.05 s, separation potential=1277 V, injected analyte concentration=1.0 m*M* in BGE and injected sample band length=222 cells (corresponding to 0.0333 cm). Simulations were carried out on a Gateway2000 P5-120 computer (Gateway, Sioux City, SD, USA) as described in [10].

3. Results and discussion

The time axis in each electropherogram has been converted to effective mobility axis (mobilities corrected for the effects of electroosmotic flow), because this way electropherograms that were obtained on capillaries of different lengths (50 cm effective

length for the measured electropherograms, 4 cm effective length for the simulations) can be compared directly. While the peak positions are invariant on the mobility scale, the peaks become broader (and the shape of the boundaries becomes less crisp) as residence time in the capillary is increased.

The measured electropherograms of the five-analyte sample are shown in Fig. 1. The test mixture contained 1 m*M* each of two $HMBTM^+$ isomers ($\mu^{eff}=31\cdot10^{-5}$ cm^2/V s and $\mu^{eff}=29\cdot10^{-5}$ cm^2/V s), one $HMBTE^+$ isomer ($\mu^{eff}=25\cdot10^{-5}$ cm^2/V s), and two $HMBTB^+$ isomers ($\mu^{eff}=21\cdot10^{-5}$ cm^2/V s and $\mu^{eff}=19\cdot10^{-5}$ cm^2/V s). The numbers on the right hand side of each electropherogram indicate the Li^+: TBA^+ ratio of the respective BGEs. The dashed lines show the angle at which the axes in the successive electropherograms are shifted up and to the right. Grossly distorted peaks are observed in all three electropherograms: the first peak in the 5:20 Li^+:TBA^+ BGE, the first and second peaks in the 10:15 BGE and the third peak in the 15:10 BGE.

The simulated analyte concentration profiles are shown in Fig. 2, the Li^+ and TBA^+ co-ion concentration change profiles in Figs. 3 and 4, the counter-ion concentration change profile in Fig. 5 and the local electric field strength change profile in Fig. 6. (The displayed change is obtained as the difference between the calculated actual value and

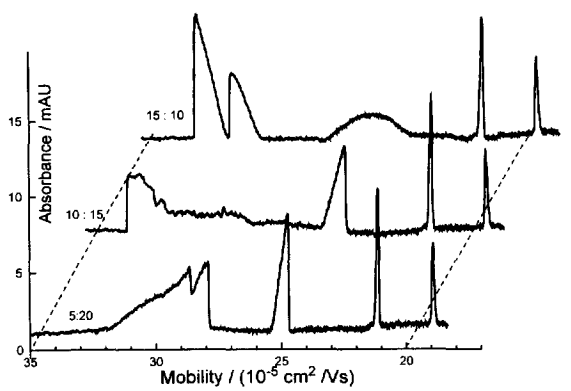

Fig. 1. Measured electropherograms for the five-analyte sample which contains 1 m*M* each of two $HMBTM^+$ isomers ($\mu^{eff}=31\cdot10^{-5}$ cm^2/V s and $\mu^{eff}=29\cdot10^{-5}$ cm^2/V s), one $HMBTE^-$ isomer ($\mu^{eff}=25\cdot10^{-5}$ cm^2/V s) and two $HMBTB^+$ isomers ($\mu^{eff}=21\cdot10^{-5}$ cm^2/V s and $\mu^{eff}=19\cdot10^{-5}$ cm^2/V s). For experimental conditions see text. The dashed lines indicate the displacement of the mobility axes in the respective electropherograms.

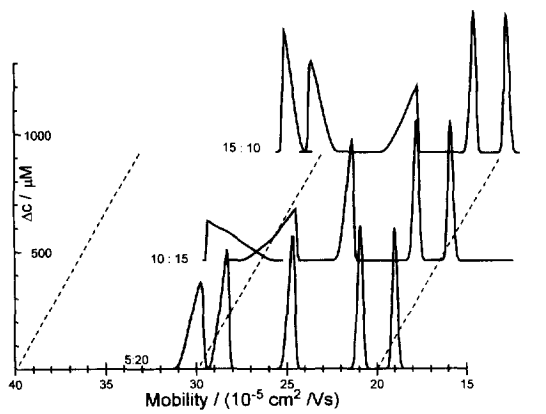

Fig. 2. Simulated electropherograms (analyte concentration traces) for the five-analyte sample in Fig. 1. For simulation conditions see text.

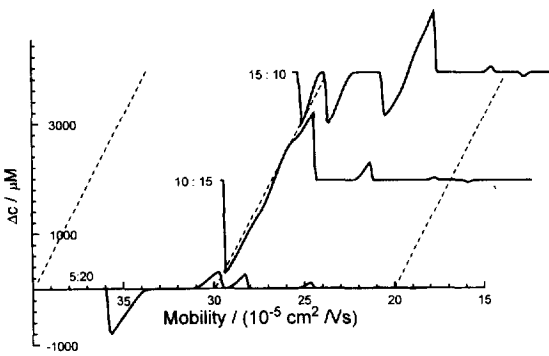

Fig. 3. Simulated Li^+ co-ion concentration change traces for the electrophoretic separation of the five-analyte sample in Fig. 1. For simulation conditions see text.

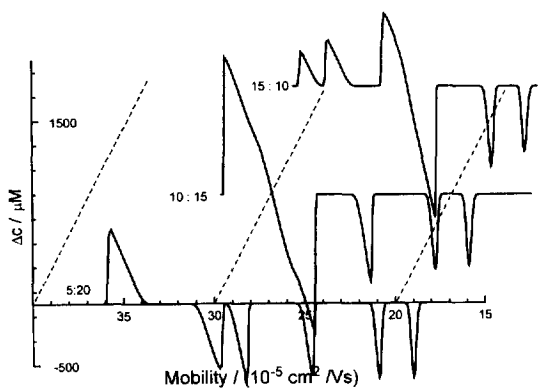

Fig. 4. Simulated TBA^+ co-ion concentration change traces for the electrophoretic separation of the five-analyte sample in Fig. 1. For simulation conditions see text.

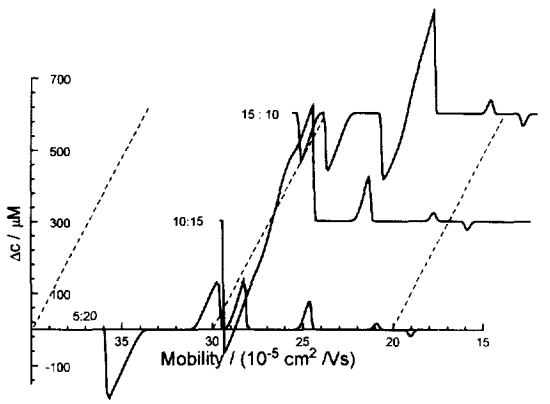

Fig. 5. Simulated counter-ion concentration change traces for the electrophoretic separation of the five-analyte sample in Fig. 1. For simulation conditions see text.

the nominal steady state value in the pure BGE zones. This way, the co-ion and counter-ion concentration traces obtained in different BGEs can be plotted on the same scale, and the relative magnitudes of the induced disturbances can be compared with each other directly.)

The analyte concentration traces (Fig. 2) indicate that all peaks front in the 5:20 BGE; the first and second peak (the two fastest peaks) show diffuse boundaries which point towards each other in the 10:15 BGE, as do the second and third peak in the 15:10 BGE. These peak patterns are in agreement with the extended peak shape rules described in [10] and can be easily interpreted once the non-comigrating system peak (the "new" peak) and the governing co-ion peak (the co-ion that together with the non-comigrating system peak, brackets the analyte in question) are located in Figs. 3–6. In the 5:20 BGE, the non-comigrating system peak is located at $35 \cdot 10^{-5}$ cm^2/V s. It is faster than any of the analytes and, together with TBA^+, brackets the analytes. Consequently, TBA^+ (at $20 \cdot 10^{-5}$ cm^2/V s) becomes the governing co-ion for all the analytes. According to the peak shape rules [10], the self-sharpening boundaries of the analytes should point toward the mobility position of the governing co-ion, TBA^+. Indeed, this is the case as shown by the 5:20 traces in both Figs. 1 and 2.

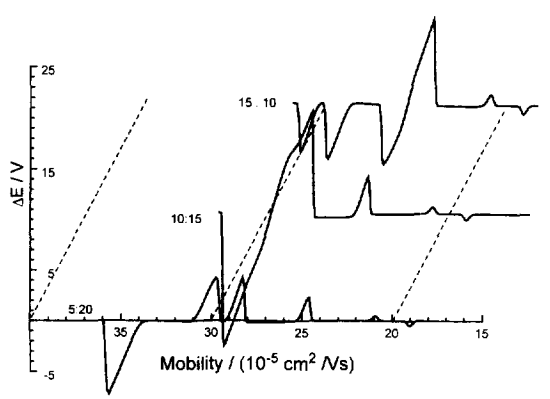

Fig. 6. Simulated electric field strength change traces for the electrophoretic separation of the five-analyte sample in Fig. 1. For simulation conditions see text.

In the 10:15 BGE, the diffuse edges of the first and second peak in Fig. 2 point towards each other. This, according to the extended peak shape rules [10], occurs when the mobility position of the non-comigrating system peak is in-between the two analyte peaks. Thus, the governing co-ion for the first peak is Li^+ (consequently, the sharp front of the analyte faces towards Li^+); the governing co-ion for the second peak (and also, for the rest of the peaks) is TBA^+ (consequently, the sharp front of these analytes face towards TBA^+). Interestingly, no clear "new" peak is discernible in the 10:15 BGE traces in Figs. 3–6 that could be identified as the non-comigrating system peak. This is so because the non-comigrating system peak occurs half-way between the second and third analyte peaks and shows up only as shoulders on both diffuse sides of the "bow-tie" shaped overlapped peak. It is not surprising that the combined width of the first and second analyte peaks is as large as 5 mobility units because, according to the extended peak shape rules, the closer the analyte peak is to the non-comigrating system peak the broader it is. This explains why the second peak appears missing (is spread out into the noise of the baseline) in the 10:15 trace in Fig. 1. In the 15:10 BGE, the diffuse edges of the second and third peak in Fig. 2 point towards each other. Again, according to the extended peak shape rules [10], this means that the mobility position of the non-comigrating system peak is in-between them; the governing co-ion for the first and second analyte peak is Li^+ (consequently, the sharp fronts of the analytes face towards Li^+). The governing co-ion for the third peak (and also, for all the other peaks) is TBA^+,

consequently, the sharp boundaries of these analytes face towards TBA^+. The non-comigrating system peak is the third peak in the 10:15 BGE traces in Figs. 3–6. Again, the combined width of the non-comigrating system peak and third analyte peak is 3.5 mobility units, which explains why the third peak in the 15:10 trace is so broad in Fig. 1.

By varying the mole ratio of the two co-ions, one can shift the position of the non-comigrating system peak into a segment of the electropherogram that does not contain analytes. This possibility is indicated in Fig. 7, which shows the measured electropherogram, the simulated analyte trace and the Li^+ trace for the 20:5 BGE. The non-comigrating system peak is the small, fourth peak in the Li^+ trace. The shifting of the mobility position of the non-comigrating system peak by the addition of a small amount of an inert salt of one of the co-ions could be a very important and powerful tool when the BGEs contain a permanently charged interacting agent (such as a charged cyclodextrin or a micellar agent), whose concentration must be maintained at a certain level to provide adequate separation selectivity, but produces an interfering non-comigrating system peak [15].

Apart from helping to locate the position of the non-comigrating system peak, the simulated Li^+ and TBA^+ traces in Figs. 3 and 4 are of special importance for indirect detection schemes which utilize one of the co-ions as indirect detection agent in two co-ion BGEs. The "cleanest", most uniform response pattern would be obtained in BGEs where the non-comigrating system peak is faster than any of the analytes, and the governing co-ion is the active detection agent. In all other combinations there will be broad sections of the mobility range that are blocked out by the induced non-comigrating system peak, whose position depends only on the mobilities and concentration ratios of the two BGE co-ions. BGEs with two detectable co-ions would generally lead to less readily interpreted (and thus inferior) indirect detector response patterns.

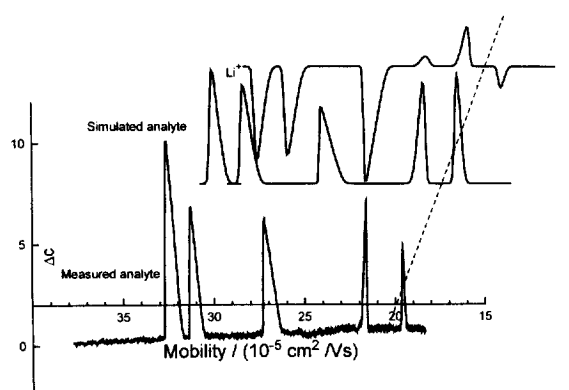

Fig. 7. Comparison of the measured and simulated analyte concentration and Li^+ concentration change traces for the 20:5 Li^+:TBA^+ BGE.

4. Conclusions

Our earlier single analyte–two co-ion electrophoretic simulations were extended to handle up to eight permanently ionic analytes in BGEs which contain two strong electrolyte co-ions. The extended peak shape rules derived from the single analyte simulations were found to apply for the multiple analyte simulations as well. A five component sample of quaternary ammonium compounds was analyzed in 25 m*M* constant ionic strength BGEs, which contained lithium and tetrabutylammonium ions in varying mole ratios as co-ions. Grossly distorted analyte peaks were observed in two of these two co-ion BGEs. Computer simulations of these systems indicated that peak distortion in both cases was caused by the overlap of the non-comigrating system peak and the analyte peak(s) and could effect mobility ranges as broad as $5 \cdot 10^{-5}$ cm^2/V s. By simply varying the mol ratio of the two co-ions, the interfering non-comigrating system peak can be shifted into "empty" sections of the electropherogram. The simulations indicate that when one of the co-ions is used as the active agent in indirect detection schemes, reasonably "clean", easily interpreted peak patterns can be obtained provided that the non-comigrating system peak is more mobile than any of the analyte peaks and the governing co-ion (slow co-ion) is the detection agent.

Acknowledgments

Partial financial support of this project by the Advanced Research Program of the Texas Coordinating Board of Higher Education (Grant No. 010366-

016), Beckman Instruments (Fullerton, CA, USA) and the R.W. Johnson Pharmaceutical Research Institute (Spring House, PA, USA) is gratefully acknowledged.

References

[1] F.E.P. Mikkers, F.M. Everaerts, Th.P.E.M. Verheggen, J. Chromatogr. 169 (1979) 1.
[2] V. Šustáček, F. Foret, P. Boček, J. Chromatogr. 545 (1991) 239.
[3] Y.Y. Rawjee, R.L. Williams, Gy. Vigh, Anal. Chem. 66 (1994) 3777.
[4] Y.Y. Rawjee, Gy. Vigh, R.L. Williams, US Pat. 5 614 072, 1997.
[5] R.L. Williams, Gy. Vigh, J. Liq. Chromatogr. 18 (1995) 3813.
[6] J. Bullock, J. Strasser, J. Snider, J. Anal. Chem. 67 (1995) 3246.
[7] R.L. Williams, Gy. Vigh, J. Chromatogr. A 730 (1996) 273.
[8] R.L. Williams, Gy. Vigh, J. Chromatogr. A 744 (1996) 75.
[9] R.L. Williams, Gy. Vigh, J. Chromatogr. A 763 (1997) 253.
[10] R.L. Williams, B. Childs, E.V. Dose, G. Guiochon, Gy. Vigh, Anal. Chem. 69 (1997) 1347.
[11] E.V. Dose, G. Guiochon, Anal. Chem. 63 (1991) 1063.
[12] B.A. Williams, Gy. Vigh, Anal. Chem. 68 (1996) 1174.
[13] B.A. Williams, Gy. Vigh, Anal. Chem. 67 (1995) 3079.
[14] J.N. Kanazawa, N.S. Nishinomiya, US Pat. 3 134 788, 1964.
[15] R.L. Williams, Gy. Vigh, in preparation.